Chinese Journal of
POLYMER SCIENCE

ARTICLE

https://doi.org/10.1007/s10118-021-2619-7
Chinese J. Polym. Sci. **2021**, *39*, 1657–1664

Liquid Crystalline Microdroplets of Graphene Oxide *via* Microfluidics

Piao Ma, Peng Li, Ya Wang, Dan Chang, Wei-Wei Gao*, and Chao Gao*

MOE Key Laboratory of Macromolecular Synthesis and Functionalization, Department of Polymer Science and Engineering, Key Laboratory of Adsorption and Separation Materials & Technologies of Zhejiang Province, Zhejiang University, Hangzhou 310027, China

Electronic Supplementary Information

Abstract Study of stable liquid crystal (LC) microdroplets is of great significance for LC dynamics in confined space or at topological surface. However, the fabrication of LC microdroplets with diverse shape without ionic gelation agents still remains challenging due to the fluid instability. Here, we utilize the microfluidic technology to prepare graphene oxide (GO) LC microdroplets with various morphologies based on the anomalous rheological property of GO aqueous dispersion. Different from LC of one-dimensional polymer, LC containing two-dimensional GO sheets exhibits considerable viscoelasticity and weak extensibility, resulting from the planar molecular conformation and the absence of intermolecular entanglements. The low extensibility ensures that GO aqueous suspension is discretized into monodispersed microdroplets rather than thin thread in the microfluidic channels. The large viscoelasticity and ultra-long relaxation time of GO LC enable the diverse stable morphologies of microdroplets. The droplet morphology is well controlled from sphere to teardrop by modulating the competition between GO viscoelasticity and interfacial tension. The two-dimensional GO LC featuring unique rheological property provides a novel system for the microfluidic field, and corresponding topological stability enriches the LC dynamics and opens a new pathway for designing graphene-based materials.

Keywords Graphene oxide; Liquid crystal; Microdroplets; Microfluidics

Citation: Ma, P.; Li, P.; Wang, Y.; Chang, D.; Gao, W. W.; Gao, C. Liquid crystalline microdroplets of graphene oxide *via* microfluidics. *Chinese J. Polym. Sci.* **2021**, *39*, 1657–1664.

INTRODUCTION

Liquid crystal (LC) is a thermodynamic metastable phase exhibiting both the anisotropy of crystalline solid and the fluidity of liquid.[1,2] Because physical, chemical and rheological properties are closely coupled with the scale, geometric and interfacial effects, complex texture and unconventional flows occur in LC at confined and topological space, such as hazelnuts droplets and jellyfishes droplets.[3–5] Liquid droplets are usually obtained by discretizing continuous fluid into independent and stable phases.[6,7] The investigation on the formation and deformation of liquid droplets is critical to related applications across distinct length scales,[8] including microcosmic fuel diffusion, cell deformation research, inkjet printing, macroscopic food processing[9] and so on.[10,11] Currently, microdroplets are primarily fabricated by microfluidic technology (MFT), which has been well developed in many fields of microprinting, heterogeneous fiber fabrication and drug delivery.[12–14] Microdroplets with different morphologies, especially non-spherical microdroplets, serve as a possible model to study the flow behavior of trace liquid and the macromolecule aggregation phenomena in confined space.[15,16] However, preparing stable non-spherical microdroplets is hard because of the fluid instability and large interfacial tension on the microscale.[17–22]

To maintain the stability of non-spherical microdroplets, appropriate liquid viscoelasticity is required for resisting the interfacial tension. Polymer solution is the most common type of viscoelastic fluid, which exhibits large intrinsic viscoelasticity and extrinsic stretchability due to the chain entanglement.[23,24] These inseparable characteristics induce the solution to become long thin threads in flow fields rather than monodisperse microdroplets. Graphene oxide (GO) is a typical two-dimensional macromolecule and its aqueous dispersion could form nematic LC phase at concentrations higher than 0.1 wt%.[25–31] Much different from one-dimensional polymer solution, GO dispersion exhibits low stretchability for the absence of intermolecular entanglement. Therefore, extensional flow field can discretize the GO LC thread into monodisperse microdroplets with non-spherical morphologies.[32,33] Previous reports have shown macroscopic non-spherical GO droplets of 2–5 mm in diameter, like GO caps droplets,[3] are stabilized by ionic gelation agents.[34–36] Ionic gelation agents made the GO droplets with poor fluidity and difficult to fuse with each other. Nevertheless, it still remains a great challenge to obtain non-spherical GO LC droplets at micron scale without adding ionic gelation agents.

In this work, we realize the fabrication of GO LC microdroplets with a series of morphologies tunable from sphere to

* Corresponding authors, E-mail: wwgao@zju.edu.cn (W.W.G.)
E-mail: chaogao@zju.edu.cn (C.G.)

Received May 12, 2021; Accepted June 11, 2021; Published online July 30, 2021

teardrop without ionic gelation agents. The morphology is adjusted by altering interfacial tension and fluidic viscoelasticity. The impact of these two factors on the microdroplet morphology is explored and the related results are summarized in a phase diagram. Customized topologies are achieved *via* fusion between multiple microdroplets, benefiting from the fluidity of GO microdroplets since the absence of curing agents. The stable GO LC microdroplets show potential in manufacturing novel graphene-based materials and provide a model to study the dynamics of two-dimensional LC in confined spatial systems.

EXPERIMENTAL

Materials

Single-layer GO sheets (≥99.5%) with an average lateral size of 30–50 μm (Fig. S1 in the electronic supplementary information, ESI) were purchased from Hangzhou Gaoxi Technology Co., Ltd. Isopar G (oil phase, C10H24) and polyacrylate sodium (PAAS) were purchased from Shanghai Salang Chemical Co., Ltd. EM90 (surfactant, Cetyl polyethylene glycol) was purchased from Evonik Industries AG. The microfluidics chip (inner channel cylindrical) was purchased from Suzhou Wenhao Technology Co., Ltd. The inner channel radius of the chip used in GO suspension is 100 μm and that in the case of GO&PAAS suspension is 37.5 μm.

Methods

To fabricate GO microdroplets, GO aqueous suspension with a certain concentration was steadily extruded from inner channel of microfluidics chip by a syringe pump. The extrusion rate of GO suspension was varied from 0.1 mL/h to 2.0 mL/h. Oil phase containing Isopar G was extruded from other channels to discretize the GO suspension and stabilize GO microdroplets. The extrusion rate of oil was varied from 10 mL/h to 70 mL/h. Surfactant of EM90 was introduced into the oil phase to adjust interfacial tension. The surfactant concentration was changed from 0 wt% to 2 wt%. The GO suspension from 2 mg/g to 9 mg/g was prepared to investigate the effect of GO concentration on the microfluidics process. In the fusion process, we used the method of solvent exchange to fabricate jointed microdroplets. The concentration of surfactant in the solvent before fusion is in the range of 1 wt%–2 wt%, and that after fusion ranges from 0 wt% to 1 wt%. The change in surfactant concentration determines the degree of fusion. As the variation of surfactant concentration gets larger, the fusion degree is higher. In the GO&PAAS system, extrusion rate of GO&PAAS composite suspension was varied from 0.5 μL/min to 1 μL/min and the extrusion rate of oil phase ranged from 30 μL/min to 120 μL/min. The surfactant concentration was constant at 1 wt%.

Characterizations

The photographs of samples were collected by a camera of Canon EOS700D. A strain-controlled rheometer (ARES-G2, TA Instruments, USA) with a steel cone-plate geometry (40 mm of diameter, 2° of cone angle, 50 μm of gap) was used to measure the rheological response of the GO aqueous suspension in steady shear. The temperature was controlled at 26 ℃ by using a Peltier system. Interfacial tension was measured at a CTS-200 system (Mighty Technology Pvt. Ltd., China). The structure of microspheres was characterized by a scanning electron microscope (SEM) (Hitachi S4800, Japan) system.

RESULTS AND DISCUSSION

Fabrication of Microdroplets

The microdroplets with adjustable aspect ratio (AR) from teardrops to spheres were fabricated according to the synergistic effect between viscoelasticity and interfacial tension. During the fabrication process, GO LC suspension and oil phase flowed respectively through two orthogonal channels in the microfluidics chip, where the flow velocity of GO suspension is lower than that of oil phase (Fig. 1a). Due to the absence of intermolecular entanglement, the GO suspension exhibits large viscoelasticity and low stretchability, which facilitates the dissociation of the suspension into monodispersed microdroplets under extensional flow (Fig. 1c). On one hand, the interfacial tension between GO aqueous suspension and oil phase makes the teardrops tend to evolve into spherical droplets. On the other hand, the intrinsic viscoelasticity of GO facilitates the preservation of the non-spherical teardrop shape (Fig. 1b). By matching the two contrary factors, the morphology of the microdroplets was tuned from sphere to teardrops (Fig. S2 in ESI). In the case of LC microdroplets made from large-sized GO platelets, great morphological stability is exhibited. The polarized optical microscopy (POM) observation revealed that the GO teardrop still maintained the intact LC texture and constant aspect ratio even after storing for ten days at room temperature despite an extremely low GO concentration (2 mg/g) (Fig. 1d and Fig. S3 in ESI).

Hydrodynamic Analysis

The hydrodynamic analysis revealed that the viscoelasticity of GO suspension and the interfacial tension between GO dispersion and oil phase were two critical factors to determine the morphology of GO LC microdroplets (Fig. 2a). The GO LC suspension formed monodispersed teardrops after being discretized by flow field. The interfacial tension (σ) at microscale is strong and drives the microdroplets to become spheres. The final microdroplet morphology is dominated by the balance of intrinsic viscoelasticity and external forces, including interfacial tension and flow extension. Viscosity (η) of GO dispersion and relative speed (v) between GO and oil phases influence the discretization and deformation processes of microdroplets. Viscosity determines the flow rate within the microdroplet bulk and relative speed effects discretization and aspect ratio of original micro-teardrop. The intrinsic viscoelasticity of GO suspension resists the flow induced by Laplace pressure and maintains the non-spherical geometry of GO microdroplets.[37–39] The influences of interfacial tension, viscosity and relative flow speed are integrated into a dimensionless capillary number (Ca):

$$Ca = \eta v/\sigma \quad (1)$$

$$v = V_1 - V_2 \quad (2)$$

where η, σ and v denote viscosity of GO suspension, interfacial tension between GO and oil phases, and relative speed between GO suspension and driving oil fluid, respectively. In addition, the extremely long relaxation time and the ultra-stable LC texture of two-dimensional GO sheets endowed GO LC with large viscoelasticity even in a dilute concentration range (below

https://doi.org/10.1007/s10118-021-2619-7

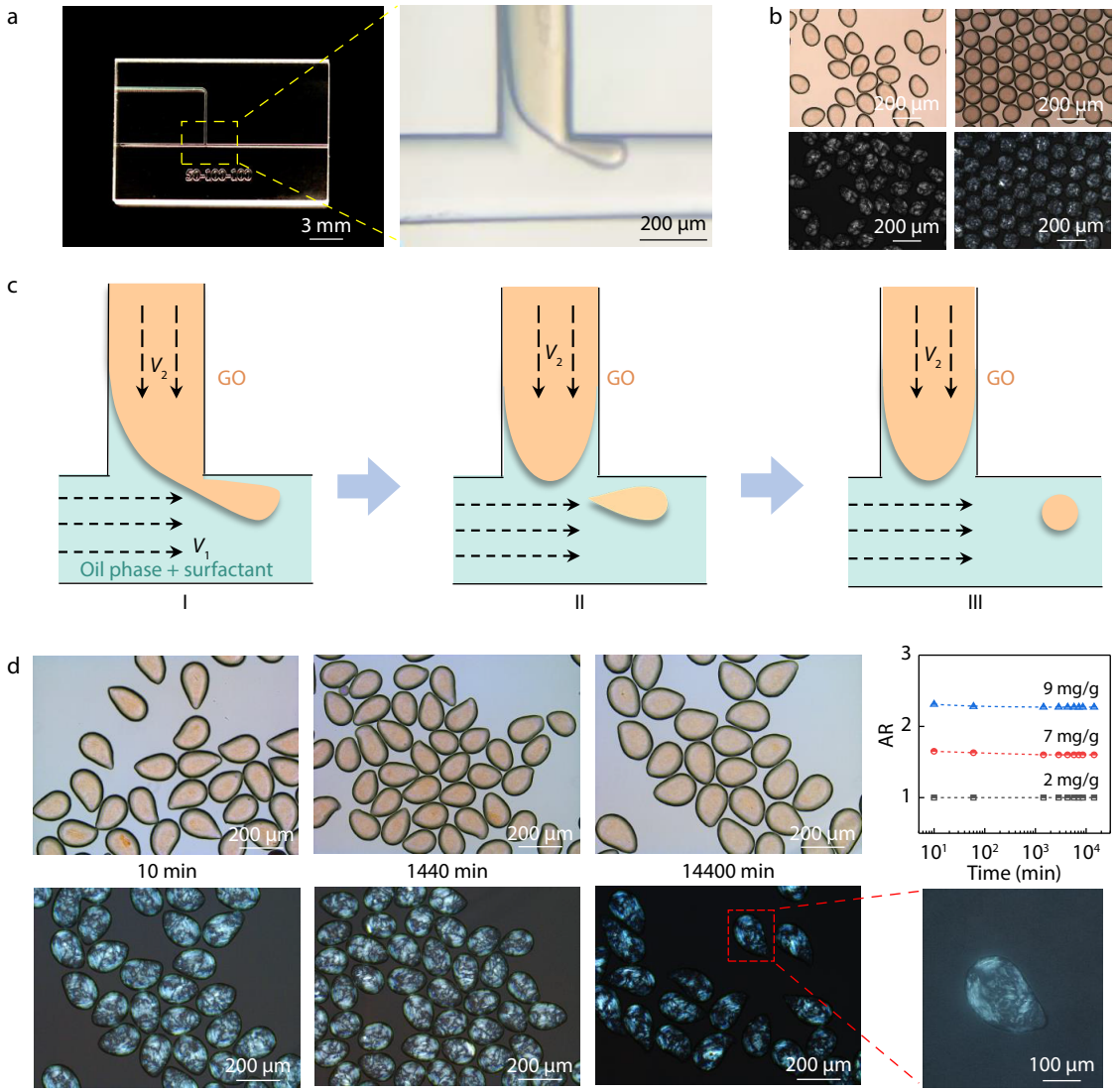

Fig. 1 Graphene oxide (GO) liquid crystal microdroplets. (a) Microfluidics chips used to fabricate GO microdroplets; (b) Optical and polarized optical images of GO microdroplets with different morphologies; (c) Scheme of the fabrication process; (d) Stability of GO microdroplets after the long-time storage. The top row is optical images and the bottom row is the corresponding polarized optical images. The aspect ratio of microdroplets was shown in the right chart.

2 mg/g) (Fig. 2b). The viscoelasticity could be reflected by the reciprocal value of loss factor ($\tan^{-1}\theta$) which is calculated by the ratio of elastic modulus (G') to loss modulus (G'').

Morphology Phase Diagram of Microdroplets

To control the morphologies of GO microdroplets, the interfacial tension was modulated by changing the content of surfactant in the oil phase and the GO viscoelasticity was tuned based on the concentration of GO suspension (Fig. 2c). Accordingly, a series of microdroplets with different aspect ratios were fabricated and a phase diagram of microdroplet morphology versus Ca and $\tan^{-1}\theta$ was obtained (Figs. 2d and 2e). The results show the morphology of GO LC microdroplets transforms from sphere to teardrop with increasing Ca and $\tan^{-1}\theta$. Here the rising Ca means the effect of interfacial tension decreases and smaller Laplace pressure was caused, while the enhanced $\tan^{-1}\theta$ indicates that stronger elasticity of GO LC was exhibited compared to viscosity as flowing. The large elasticity resists the Laplace pressure caused by interfacial tension and is favorable to the preservation of non-spherical morphology formed by GO LC.

To further prove the rheological deduction, we compared the morphologies of GO LC microdroplets made by a lower concentration with that by 9 mg/mL. The concentration of GO suspension was diluted stepwise from 9 mg/mL to 2 mg/mL. The optical images from 9 mg/mL to 2 mg/mL are shown in Figs. 3(a) and 3(b). Corresponding microdroplets still displayed the LC texture under polarized optical microscope (Figs. 3c and 3d). The interfacial tension between GO dispersion and oil phase was calculated to change from 7.56 mN/m to 5 mN/m. Additionally, the velocity ratio of oil phase to GO suspension was tuned from 30 to 50. In the case of GO suspension of 2 mg/mL, GO LC microdroplets formed sphere at different velocity ratios even under a small interfacial tension

https://doi.org/10.1007/s10118-021-2619-7

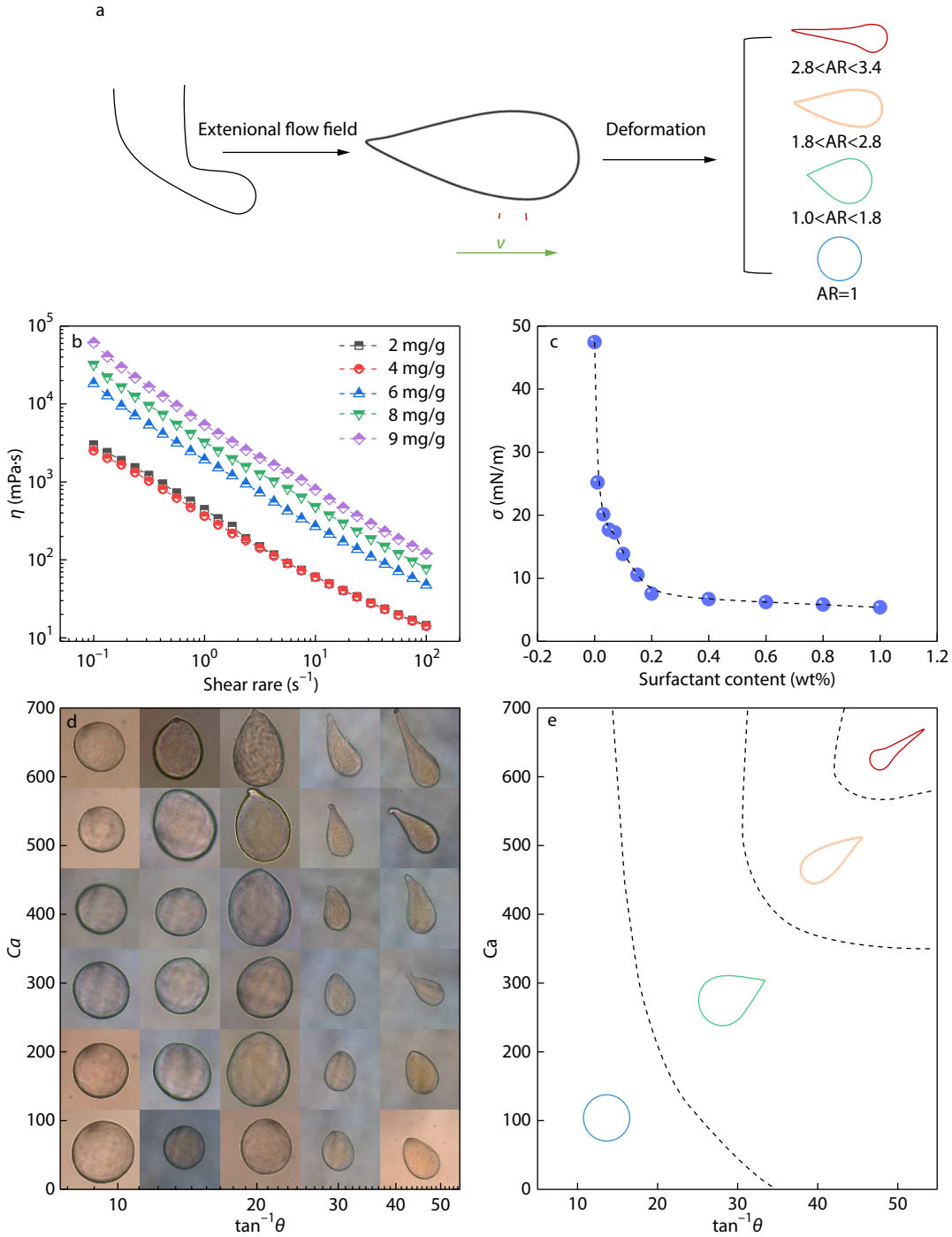

Fig. 2 Hydrodynamic analysis and morphology controlling of GO LC microdroplets. (a) Synergistic effect of external forces and internal rheological property (speed ratio v, viscosity η, interface tension σ and viscoelasticity $\tan^{-1}\theta$) during the fabrication process; (b) Viscosity of GO suspension with different concentrations; (c) Interfacial tension with surfactant content; (d) Optical images of GO microdroplets with different Ca and $\tan^{-1}\theta$; (e) GO LC microdroplets phase diagram extracted from (d).

of 5 mN/m (Figs. 3b and 3d). While GO microdroplet made from a higher concentration of 9 mg/mL became teardrop in the appropriate range of interfacial tension. This result illustrates the stability of non-spherical droplets increases with rising viscoelasticity of GO phase (Figs. 3b and 3c). In addition, the velocity ratio was found to not affect the morphology and LC texture of microdroplets (Figs. S4–S8 in ESI).

Characterization of Single LC Microdroplet

The intrinsic structure of GO microdroplets was characterized by freeze-drying strategy, in which the corresponding morphologies and structures were retained (Fig. S9 in ESI). The intact morphology and texture of GO sheets were further confirmed by SEM observation. Moreover, GO layers were found to align along the surface of spherical microdroplets (~1 in AR)

https://doi.org/10.1007/s10118-021-2619-7

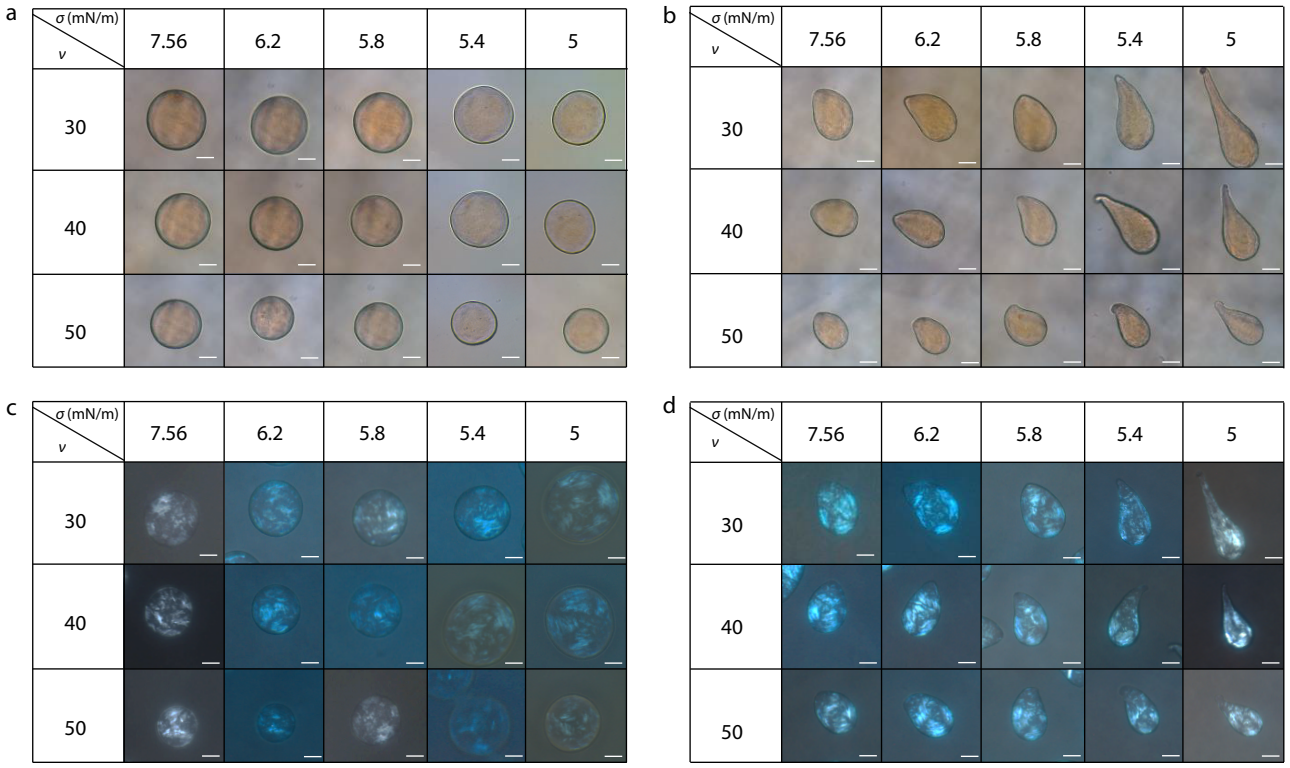

Fig. 3 Optical and polarized optical images of GO droplets with different concentrations. (a) Images of low-concentration GO LC microdroplets with different speed ratios (*v*) and interface tensions (*σ*). GO concentration was 2 mg/g; (b) Images of GO LC high-concentration microdroplets with different speed ratios (*v*) and interfacial tensions (*σ*). GO concentration was 9 mg/g; (c) Polarized optical images corresponding to (a). (d) Polarized optical images corresponding to (b). Scar bars are 50 μm.

that have a high GO content. The layer-by-layer stacking of GO sheets is mainly parallel to the spherical surface, demonstrating the onion-like architecture of microspheres (Fig. 4a). In comparison, only a few layers of GO orient along the surface of teardrop microdroplets which were fabricated with the same GO concentration (Fig. 4b). The anomalous GO arrangement of teardrop shape could be attributed to the symmetry breaking of microdroplets. The asymmetrical morphology induces confinement of GO platelets, thereby affecting the related alignment within the LC teardrop. These control experiments show that the LC texture is indeed relevant to the morphology of liquid droplets. Further decrease in the GO concentration leads to a declined stacking order in spherical microdroplets while an enhanced alignment along the surface of teardrop shape. For the teardrop case, the arrangement of GO layers along the long axis presents quasi-nematic phase. This order suggests that asymmetrically confined space may cause partial orientation of GO sheets along the dominated geometrical direction. Thus, this work revealed the key role of morphology in the condensed state of molecules at microscale, which enriches the study of LC dynamics in asymmetrical confined spaces.

Assembly of Multiple LC Microdroplets

On the basis of the excellent stability, multiple LC microdroplets were assembled into a two-dimensional superlattice. The spherical microdroplets orderly stacked into an anisotropic lattice, exhibiting the potential in the assembled micropatterns and microprinting. After increasing the AR of microdroplet, the symmetry of building blocks was broken and the perfect long-range order was destroyed. Therefore, the microdroplets organized into two-dimensional quasi-lattices. When the aspect ratio was further increased, the droplet array became isotropic, resulting from the random arrangement of individuals (Fig. 4c). Overall, the GO LC microdroplets with various morphologies can serve as a new system to study the impact of individual geometry on the corresponding two-dimensional stacking.

Besides, diverse jointed structures of microdroplets were designed. As the prepared microdroplets were transferred into the oil phase with a lower surfactant content, the droplet stability was greatly weakened because of a larger interfacial tension. Thus, they coalesced with each other, analogous to the process of cell fusion.[40,41] The architecture of jointed microdroplets was controlled and modulated into different forms. The extremely long relaxation time of GO sheets also endowed the fused droplets with good stability. This design promises the potential to fabricate the graphene-based materials with tunable structures (Fig. 4d and Fig. S10 in ESI).

GO/PAAS Microdroplets

Since the crucial role of viscoelasticity in the microdroplet morphology, the viscoelasticity of aqueous dispersion was further altered by using 70 wt% GO and 30 wt% polyacrylate sodium (PAAS) mixture suspension (Fig. 5a). After adding the high molecular weight PAAS into GO phase, the stretchability of suspension significantly increases due to the chain entanglement-induced high viscoelasticity of PAAS. Under the extensional flow in microchannels, the GO/PAAS mixture was

https://doi.org/10.1007/s10118-021-2619-7

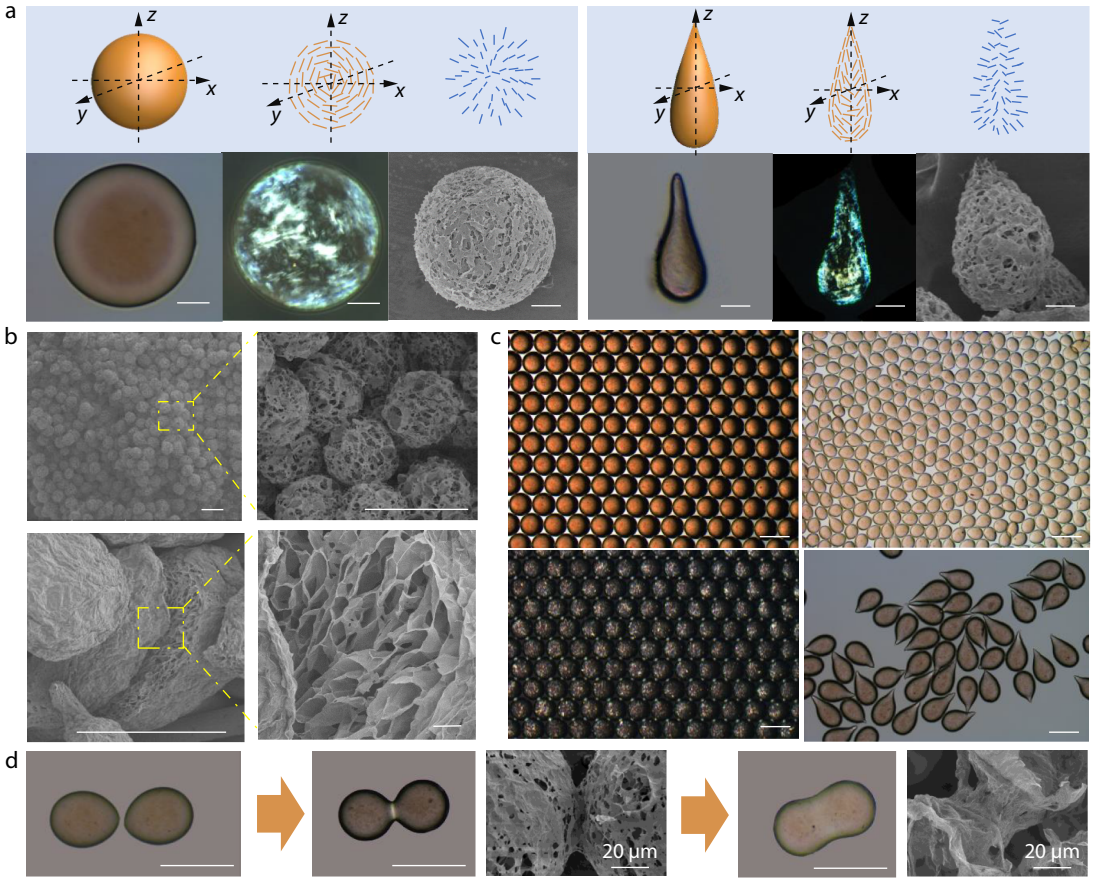

Fig. 4 Texture and architecture of GO LC microdroplets. (a) Top row: three dimensional shapes, orientation of GO sheets in cross-section profiles and cross-section director fields. Bottom row: corresponding optical images, polarized optical images and SEM images; (b) SEM images of GO LC micro aerogel with different morphologies; (c) Self-assembly of GO LC microdroplets of different aspect ratios; (d) Jointed microdroplets. Scale bars are 200 μm.

stretched into a long and thin thread with beads-on-a-string structure (Fig. S11 in ESI). There are a few microbeads and numerous nanobeads bunched between the successive microbeads on the thread. This character is much different from that of neat GO suspension. The unique structure originates from the synergistic effect of interfacial tension, viscoelasticity, and extensional flow field. After the thread pinched off, a mixture of nanodroplets and microdroplets was formed (Fig. 5b). In the initial state, the nanobeads surrounded the microbeads to form a galaxy structure. Subsequently, the nanobeads deviated from the microbeads *via* Brownian motion. In order to study the component of the beads with two size scales, polarized optical microscopy observation was applied. It can be found that the microbeads show the LC texture, while the nanobeads appear dark. The distinction in LC property indicates that phase separation in the GO and PAAS mixture occurs during the process of beads-on-a-string formation. The phase separation was possibly induced by the giant size and intrinsic elasticity of GO sheets. For the nanodroplets, large GO platelets tend to be greatly compressed and folded which results in a large elasticity within GO sheets. The intrinsic elasticity resists the external compression, leading to the expulsion of GO from the GO and PAAS mixture in nanodroplets and phase separation.

CONCLUSIONS

In conclusion, we proposed a MFT strategy to fabricate GO LC microdroplets with different morphologies. The morphology of GO microdroplets was tuned and stabilized by balancing the viscoelasticity and external force of GO, rather than introducing ionic gelation. Different from one-dimensional polymers, the aqueous suspension of two-dimensional GO sheets exhibited great viscoelasticity and low stretchability due to the absence of intermolecular entanglement. The unique rheological properties ensured GO suspension to be discretized into monodispersed microdroplets instead of long thread. In addition, the large viscoelasticity of GO suspension resisted the external force, especially interfacial tension, and stabilized the morphology of GO LC microdroplets from sphere to teardrop. The structure of microdroplets was studied by polarized optical microscopy and SEM observations. It was proved that the geometrical morphology of fluid could affect the condensed state of GO nanosheets in confined space. Additionally, the potential applications of stable GO LC microdroplets were illustrated by fabricating two-dimensional superlattice and fused GO LC architectures. To further extend the strategy of LC microdroplet preparation, PAAS was introduced into GO suspension. After adding PAAS, the viscoelasticity of aqueous phase changed and

https://doi.org/10.1007/s10118-021-2619-7

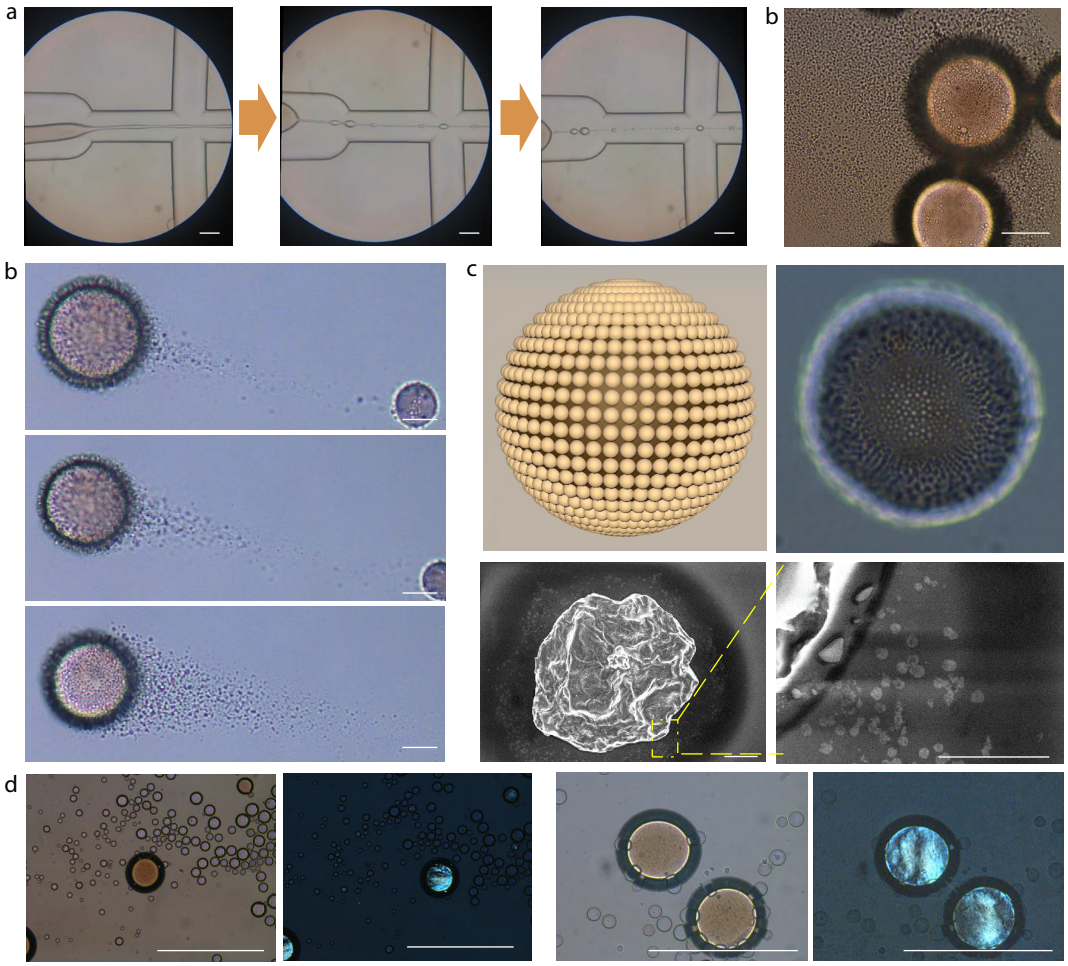

Fig. 5 Microdroplets and phase separation of GO/PAAS mixture. (a) Fabrication process of GO/PAAS mixture by microfluidics; (b) Optical image of microbeads surrounded by nanobeads; (c) Optical images of nanodroplets surrounding microdroplets. Top row: sketch diagram of beads-on-beads structure and optical image. Bottom row was SEM images; (d) Optical and polarized optical images of nanobeads and microbeads. Scale bars are 10 μm.

the unique phase separation behavior was observed. The GO LC with unique rheological properties provides a new system for microfluidic field, and the stable GO LC topology enriches the study of LC dynamics and the design of novel graphene-based materials.

Electronic Supplementary Information

Electronic supplementary information (ESI) is available free of charge in the online version of this article at http://doi.org/10.1007/s10118-021-2619-7.

ACKNOWLEDGMENTS

This work was financially supported by the National Natural Science Foundation of China (Nos. 52090030, 51533008, 51703194, 51973191, 51873191 and 51803177), National Key R&D Program of China (No. 2016YFA0200200), Hundred Talents Program of Zhejiang University (No. 188020*194231701/113), Key Research and Development Plan of Zhejiang Province (2018C01049), the Fundamental Research Funds for the Central Universities (No. K20200060) and Key Laboratory of Novel Adsorption and Separation Materials and Application Technology of Zhejiang Province (No. 512301- I21502).

REFERENCES

1 Dutta, D.; Fruitwala, H.; Kohli, A.; Weiss, R. A. Polymer blends containing liquid crystals: a review. *Polym. Eng. Sci.* **1990**, *30*, 1005–1018.
2 Stevenson, C. L.; Bennett, D. B.; Lechuga-Ballesteros, D. Pharmaceutical liquid crystals: the relevance of partially ordered systems. *J. Pharm. Sci.* **2010**, *94*, 1861–1880.
3 Yang, Q.; Jiang, Y.; Fan, D.; Zheng, K.; Zhang, J.; Xu, Z.; Yao, W.; Zhang, Q.; Song, Y.; Zheng, Q.; Fan, L.; Gao, W.; Gao, C. Nonsphere drop impact assembly of graphene oxide liquid crystals. *ACS Nano* **2019**, *13*, 8382–8391.
4 Hamlington, B. D.; Steinhaus, B.; Feng, J. J.; Link, D.; Shelley, M. J.; Shen, A. Q. Liquid crystal droplet production in a microfluidic device. *Liq. Cryst.* **2007**, *34*, 861–870.
5 Zhang, C. X.; Li, Z. F.; Zhou, Q. F.; Zhou, H. B. Study on liquid crystal polymers with two-dimensional mesogenic units. *Chinese J. Polym. Sci.* **1993**, *11*, 348–353.
6 Bollhorst, T.; Rezwan, K.; Maas, M. Colloidal capsules: nano- and

microcapsules with colloidal particle shells. *Chem. Soc. Rev.* **2017**, *46*, 2091–2126.
7 Cira, N. J.; Benusiglio, A.; Prakash, M. Vapour-mediated sensing and motility in two-component droplets. *Nature* **2015**, *519*, 446–450.
8 Xin, G.; Zhu, W.; Deng, Y.; Cheng, J.; Zhang, L. T.; Chung, A. J. Microfluidics-enabled orientation and microstructure control of macroscopic graphene fibres. *Nat. Nanotechnol.* **2019**, *14*, 168–175.
9 Dickinson, E. Stabilising emulsion-based colloidal structures with mixed food ingredients. *Sci. Food Agric.* **2013**, *93*, 710–721.
10 Chen, L. J.; Gong, L. L.; Lin, Y. L.; Jin, X. Y.; Li, H. Y.; Li, S. S.; Che, K. J.; Cai, Z. P.; Yang, C. J. Microfluidic fabrication of cholesteric liquid crystal core-shell structures toward magnetically transportable microlasers. *Lab. Chip.* **2016**, *16*, 1206–13.
11 Tomasz, S. K.; Ott, S.; Piotr, G. Droplet microfluidics for microbiology: techniques, applications and challenges. *Lab. Chip.* **2016**, *16*, 2168–2187.
12 Steinhaus, B.; Shen, A. Q.; Sureshkumar, R. Dynamics of viscoelastic fluid filaments in microfluidic devices. *Phys. Fluids* **2007**, *19*, 5.
13 Geschiere, S. D.; Ziemecka, I.; Steijn, V.; Koper, G. J.; Esch, J. H.; Kreutzer, M. T. Slow growth of the Rayleigh-Plateau instability in aqueous two phase systems. *Biomicrofluidics* **2012**, *6*, 22007–2200711.
14 Park, J. Y.; Suh, K. Y.; Seo, S. M.; Lee, H. H. Anisotropic rupture of polymer strips driven by rayleigh instability. *J. Chem. Phys.* **2006**, *124*, 214710.
15 Fang, W. Z.; Peng, L.; Liu, Y. J.; Wang, F.; Gao, C. A review on graphene oxide two-dimensional macromolecules: from single molecules to macro-assembly. *Chinese J. Polym. Sci.* **2020**, *39*, 267–308.
16 Xu, J. H.; Li, S. W.; Tan, J.; Wang, Y. J.; Luo, G. S. Preparation of highly monodisperse droplet in a T-junction microfluidic device. *Aiche J.* **2006**, *52*, 3005–3010.
17 Downs, F. G.; Lunn, D. J.; Booth, M. J.; Sauer, J. B.; Bayley, H. Multi-responsive hydrogel structures from patterned droplet networks. *Nat. Chem.* **2020**, *12*, 363–371.
18 Jiang, Y.; Guo, F.; Xu, Z.; Gao, W.; Gao, C. Artificial colloidal liquid metacrystals by shearing microlithography. *Nat. Commun.* **2019**, *10*, 4111.
19 Yeo, S. J.; Oh, M. J.; Jun, H. M.; Lee, M.; Bae, J. G.; Kim, Y.; Park, K. J.; Lee, S.; Lee, D.; Weon, B. M. A plesiohedral cellular network of graphene bubbles for ultralight, strong, and superelastic materials. *Adv. Mater.* **2018**, *30*, 1802997.
20 Mei, S.; Feng, X.; Jin, Z. Fabrication of polymer nanospheres based on rayleigh instability in capillary channels. *Macromolecules* **2011**, *44*, 1615–1620.
21 Xia, J. H.; Jiang, Y.; Gong, S. H.; Sun, Z.; Wang. Y. H. Effects of side chains with similar lengths and different structures of polyimides on liquid crystal alignment behavior. *Chinese J. Polym. Sci.* **2014**, *32*, 1610–1619.
22 Kadam, N. R. Non-spherical polymersomes: formation and characterization. *J. Pharmaceut. Biomed.* **2015**, *8*, 13–19.
23 Christopher, G. F.; Anna, S. L. Microfluidic methods for generating continuous droplet streams. *J. Phy. D. Appl. Phys.* **2007**, *40*, 319–336.
24 Wang, W. C.; Pan, Y. X.; Shi, K.; Peng, C.; Jia, X. L. Hierarchical porous polymer beads prepared by polymerization-induced phase separation and emulsion-template in a microfluidic device. *Chinese J. Polym. Sci.* **2014**, *32*, 1646–1654.
25 Sengupta, A.; Herminghaus, S.; Bahr, C. Liquid crystal microfluidics: surface, elastic and viscous interactions at microscales. *Liq. Cryst. Rev.* **2014**, *2*, 73–110.
26 Yao, B.; Chen, J.; Huang, L.; Zhou, Q.; Shi, G. Base-induced liquid crystals of graphene oxide for preparing elastic graphene foams with long-range ordered microstructures. *Adv. Mater.* **2016**, *28*, 1623–1629.
27 Zhu, P. G.; Wang, L. Q. Passive and active droplet generation with microfluidics: a review. *Lab. Chip.* **2017**, *17*, 34–75.
28 Ji, E. K.; Han, T. H.; Sun, H. L.; Ju, Y. K.; Sang, O. K. Graphene oxide liquid crystals. *Angew. Chem. Int. Ed.* **2011**, *50*, 3043–3047.
29 Xu, Z.; Gao, C. Aqueous liquid crystals of graphene oxide. *ACS Nano* **2011**, *5*, 2908.
30 Yao, W.; Mao, R.; Gao, W.; Chen, W.; Xu, Z.; Gao, C. Piezoresistive effect of superelastic graphene aerogel spheres. *Carbon* **2020**, *158*, 418–425.
31 Zhao, X.; Yao, W.; Gao, W.; Chen, H.; Gao, C. Wet-spun superelastic graphene aerogel millispheres with group effect. *Adv. Mater.* **2017**, *29*, 1701482.
32 Lopez-Polin, G.; Gomez-Navarro, C.; Parente, V.; Guinea, F.; Gomez-Herrero, J. Increasing the elastic modulus of graphene by controlled defect creation. *Nat. Phys.* **2015**, *11*, 26–31.
33 Xu, Z.; Gao, C. Graphene in macroscopic order: liquid crystals and wet-spun fibers. *Acc. Chem. Res.* **2014**, *47*, 1267–76.
34 Lv, L.; Zhang, P.; Cheng, H.; Zhao, Y.; Zhang, Z.; Shi, G. Solution-processed ultraelastic and strong air-bubbled graphene foams. *Small* **2016**, *12*, 3229–1629.
35 Ho, D. H.; Jun, H. M.; Yeo, S. J.; Hong, P.; Oh, M. J.; Weon, B. M.; Lee, W. B. Ultralightweight strain-responsive 3D graphene network. *J. Phys. Chem. C* **2019**, *123*, 9884–9893.
36 Jiang, Y.; Wang, Y.; Xu, Z.; Gao, C. Conformation engineering of two-dimensional macromolecules: a case study with graphene oxide. *Acc. Chem. Res.* **2020**, *1*, 175–187.
37 Sheng, J. J. Preferred calculation formula and buoyancy effect on capillary number: discussion of capillary number. *Asia-Pacific J. Chem. Eng.* **2015**, *10*, 25–47.
38 Li, P.; Yang, M.; Liu, Y.; Qin, H.; Liu, J.; Meng, F.; Lin, J.; Wang, F.; Gao, C. Continuous crystalline graphene papers with gigapascal strength by intercalation modulated plasticization. *Nat. Commun.* **2020**, *11*, 2645.
39 Wang, Y.; Wang, S.; Li, P.; Rajendran, S.; Xu, Z.; Liu, S.; Gou, F.; He, Y.; Li, Z.; Xu, Z.; Gao, C. Conformational scaling relations of two-dimensional macromolecular graphene oxide in solution. *Matter* **2020**, *3*, 230–245.
40 Pawar, A. B.; Caggioni, M.; Ergun, R.; Hartel, R. W.; Spicer, P. T. Arrested coalescence in pickering emulsions. *Soft Matter* **2011**, *7*, 7710.
41 Caggioni, M.; Bayles, A. V.; Lenis, J.; Furst, E. M.; Spicer, P. T. Interfacial stability and shape change of anisotropic endoskeleton droplets. *Soft Matter* **2014**, *10*, 7647.

https://doi.org/10.1007/s10118-021-2619-7